

Activity of Gut-Derived Nisin-like Lantibiotics against Human Gut Pathogens and Commensals

Zhenrun J. Zhang,^{*,#} Chunyu Wu,[#] Ryan Moreira, Darian Dorantes, Téa Pappas, Anitha Sundararajan, Huaiying Lin, Eric G. Pamer,^{*} and Wilfred A. van der Donk^{*}



Cite This: *ACS Chem. Biol.* 2024, 19, 357–369



Read Online

ACCESS |



Metrics & More

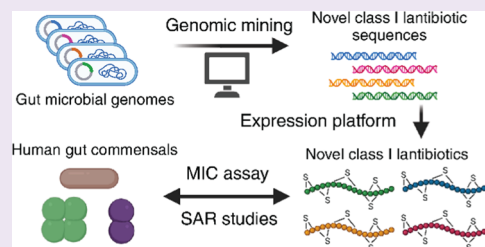


Article Recommendations



Supporting Information

ABSTRACT: Recent advances in sequencing techniques unveiled the vast potential of ribosomally synthesized and post-translationally modified peptides (RiPPs) encoded in microbiomes. Class I lantibiotics such as nisin A, widely used as a food preservative, have been investigated for their efficacy in killing pathogens. However, the impact of nisin and nisin-like class I lantibiotics on commensal bacteria residing in the human gut remains unclear. Here, we report six gut-derived class I lantibiotics that are close homologues of nisin, four of which are novel. We applied an improved lantibiotic expression platform to produce and purify these lantibiotics for antimicrobial assays. We determined their minimal inhibitory concentration (MIC) against both Gram-positive human pathogens and gut commensals and profiled the lantibiotic resistance genes in these pathogens and commensals. Structure–activity relationship (SAR) studies with analogs revealed key regions and residues that impact their antimicrobial properties. Our characterization and SAR studies of nisin-like lantibiotics against both pathogens and human gut commensals could shed light on the future development of lantibiotic-based therapeutics and food preservatives.



INTRODUCTION

Bacteria have evolved in an intense competition with other microbes in complex environments. In order to make niche clearance or to establish colonization resistance in the community, many bacteria produce bacteriocins to kill microbial competitors.¹ Bacteriocins can function as natural food preservatives through the inhibition of pathogenic bacteria, ultimately contributing to food safety.² Ribosomally synthesized and post-translationally modified peptides (RiPPs) are a major class of bacteriocins that exhibit a broad spectrum of antimicrobial activities against Gram-positive and Gram-negative bacteria including *Staphylococcus aureus*, *Enterococcus faecalis*, and *Escherichia coli*.^{3–5} The biosynthesis of RiPPs starts with a gene-encoded precursor peptide, which comprises a C-terminal core peptide fused to an N-terminal leader peptide.⁶ The leader peptide is recognized by modification enzymes that are usually encoded in the same biosynthetic gene cluster (BGC) to receive post-translational modifications on the core peptide. Subsequently, the leader peptide is removed by protease cleavage to yield the mature peptide with desired bioactivity.^{7,8} Bioinformatic studies have found great potential for RiPP discovery from the microbiome.⁹ Recent advances in metagenomic sequencing and assembly have made vast amounts of environmental microbial genomes available for investigation. Mining algorithms of BGCs with machine learning are also developed to accommodate rapidly increasing metagenomic data sets.^{7,10} Lanthipeptides are a very large family of RiPPs that are characterized by thioether cross-links called lanthionine and methyllanthionine.¹¹ The bioinformatic

tool Rapid ORF Description & Evaluation Online (RODEO)¹² has been used to discover novel lanthipeptide families from more than 100 000 genomes.¹³

Lantibiotics, coined by combining “lanthipeptide” and “antibiotics”, are a class of RiPPs that have garnered significant attention due to their potent antimicrobial properties and wide application in the food industry. The thioether macrocycles in class I lantibiotics are installed in a two-step process.¹¹ LanB dehydrates Ser and Thr residues in the LanA precursor peptides to generate dehydroalanine (Dha) and dehydrobutyrine (Dhb), respectively. The dehydration is followed by LanC catalyzing the intramolecular Michael-type addition of Cys residues to Dha or Dhb, forming lanthionine or methyllanthionine. The catalytic activity of LanB depends on glutamyl-tRNA synthetase (GluRS) and tRNA^{Glu},¹⁴ and LanBs display sequence selectivity toward the tRNA^{Glu} acceptor stem.¹⁵ Previous studies have demonstrated that introducing GluRS and tRNA^{Glu} from the native lanthipeptide-producing organism could improve the production of fully modified peptides in *E. coli*.^{15,16} Using this information, an improved production platform has been established for facile production of class I lanthipeptides in *E. coli*.¹⁷

Received: September 17, 2023

Revised: December 12, 2023

Accepted: January 10, 2024

Published: January 31, 2024



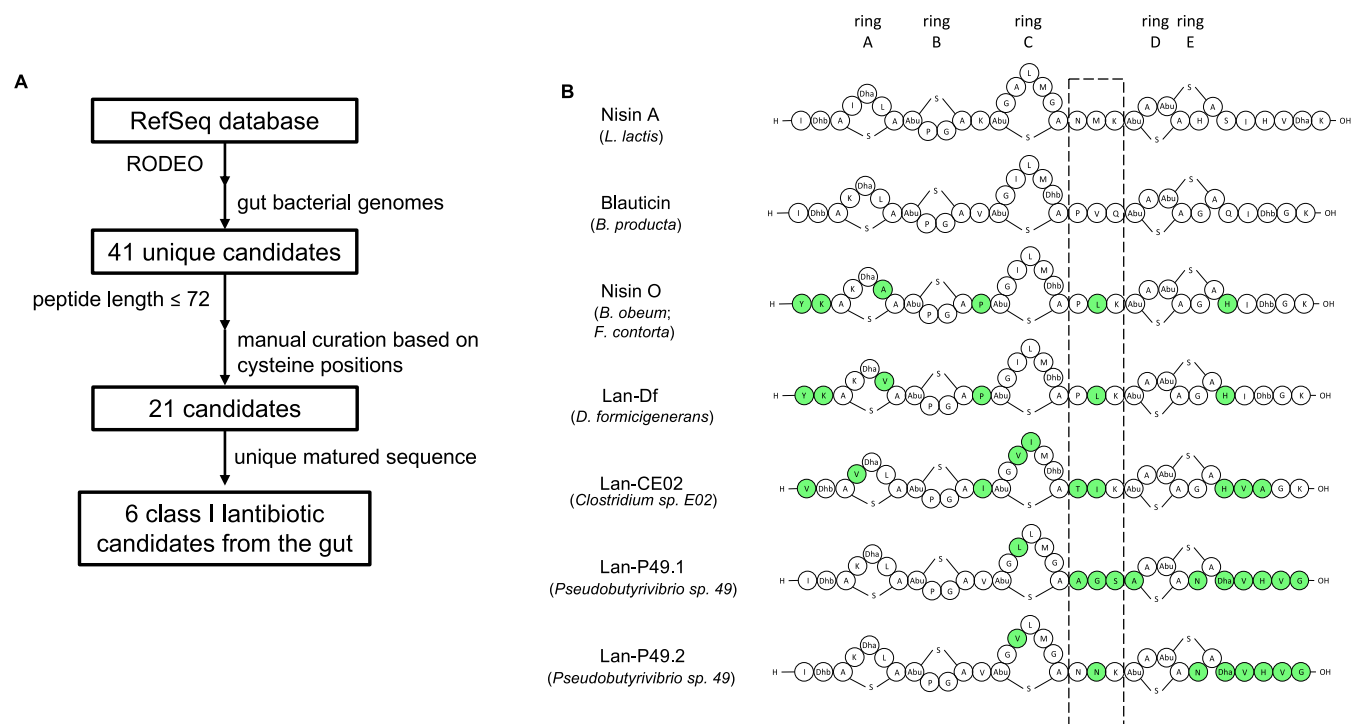


Figure 1. Bioinformatic discovery of nisin-like class I lantibiotics encoded in gut bacteria. (A) Workflow chart of lantibiotic discovery from RefSeq database using RODEO and filtering criteria. (B) Illustration of discovered putative class I lantibiotics with the ring patterns predicted based on that of nisin A. Green shading indicates residues different from both nisin A and blauticin. The dashed box indicates the hinge region. Ring designations in the structure are denoted on the top.

Blauticin, a class I lantibiotic produced by the gut commensal bacteria *Blautia producta* SCSK (BP_{SCSK}), exerts colonization resistance and clearance of vancomycin-resistant *Enterococci* (VRE) in vivo.¹⁸ A previous study showed that the in vivo VRE colonization in colon was inhibited by BP_{SCSK} but not by *Lactococcus lactis*, the producing strain of the well-studied class I lantibiotic nisin.¹⁸ In comparison to nisin, blauticin has reduced activity against intestinal commensal bacteria in vitro.¹⁸ Nisin binds lipid II and inhibits peptidoglycan biosynthesis through its N-terminal rings, and forms pores in the bacterial membrane that also involves the C terminus of the peptide.^{19–21} These pores are made up of eight nisin molecules and four lipid II molecules.²² Extensive efforts have been made to reveal the structure–activity relationship (SAR) of nisin and its antimicrobial efficacy.^{23–25} However, the SAR of blauticin and its bioactivities against pathogens and human gut commensals remain to be elucidated.

The sensitivity of human gut commensals to nisin that is widely present in food²⁶ has been surprisingly underexplored. Gram-positive human gut commensals, especially those within the Lachnospiraceae family of Bacillota (previously Firmicutes), are major producers of secondary metabolites such as short-chain fatty acids and secondary bile acids, which are crucial in contributing to the stability of the gut microbiome and host immune homeostasis.²⁷ Orally ingested nisin A induced sizable but reversible changes in microbial composition and metabolic activities of the gut microbiome in pigs²⁸ and in mice.²⁹ SAR studies of lantibiotics including blauticin and their potencies on human gut commensals will guide the future potential development of novel preservatives that could cause less collateral damage to human microbial communities. Genetic screening in pathogens and lantibiotic-producing organisms has identified multiple mechanisms of resistance

against lantibiotics. These include cell wall modifications, cell membrane modifications, and efflux pumps, among others.³⁰ However, whether these mechanisms exist in human gut commensals and how they may impact lantibiotic resistance in human gut commensals remain to be studied.

Here, we applied RODEO to the public RefSeq database to uncover novel nisin-like class I lantibiotics encoded in gut microbial genomes. After applying filtering criteria, six gut-derived class I lantibiotics that are close homologues of nisin were discovered, four of which were new. We applied the improved lantibiotic expression platform to produce and purify these lantibiotics for antimicrobial assays and determined their minimal inhibitory concentration (MIC) against both Gram-positive human pathogens and gut commensals. Furthermore, we profiled the lantibiotic resistance genes in these pathogens and commensals. Detailed SAR studies with the nisin-like analogs revealed key regions and residues in these lantibiotics that impact the antimicrobial properties. Our characterization and SAR studies of class I lantibiotics against both pathogens and human gut commensals could shed light on the future development of lantibiotic-based therapeutics and food preservatives.

RESULTS

Mining of Class I Lantibiotics from the Gut. To find novel class I lantibiotic sequences from the gut, we adopted a workflow shown in Figure 1A. We applied RODEO,¹² an algorithm previously used to identify lanthipeptide sequences in large numbers of genomes,¹³ to the RefSeq database. RODEO uses a hidden Markov model to mine for RiPP BGCs and predict precursor peptides by the combination of heuristic scoring and machine learning.¹² We restricted our search to bacterial genomes whose representatives were reported to be

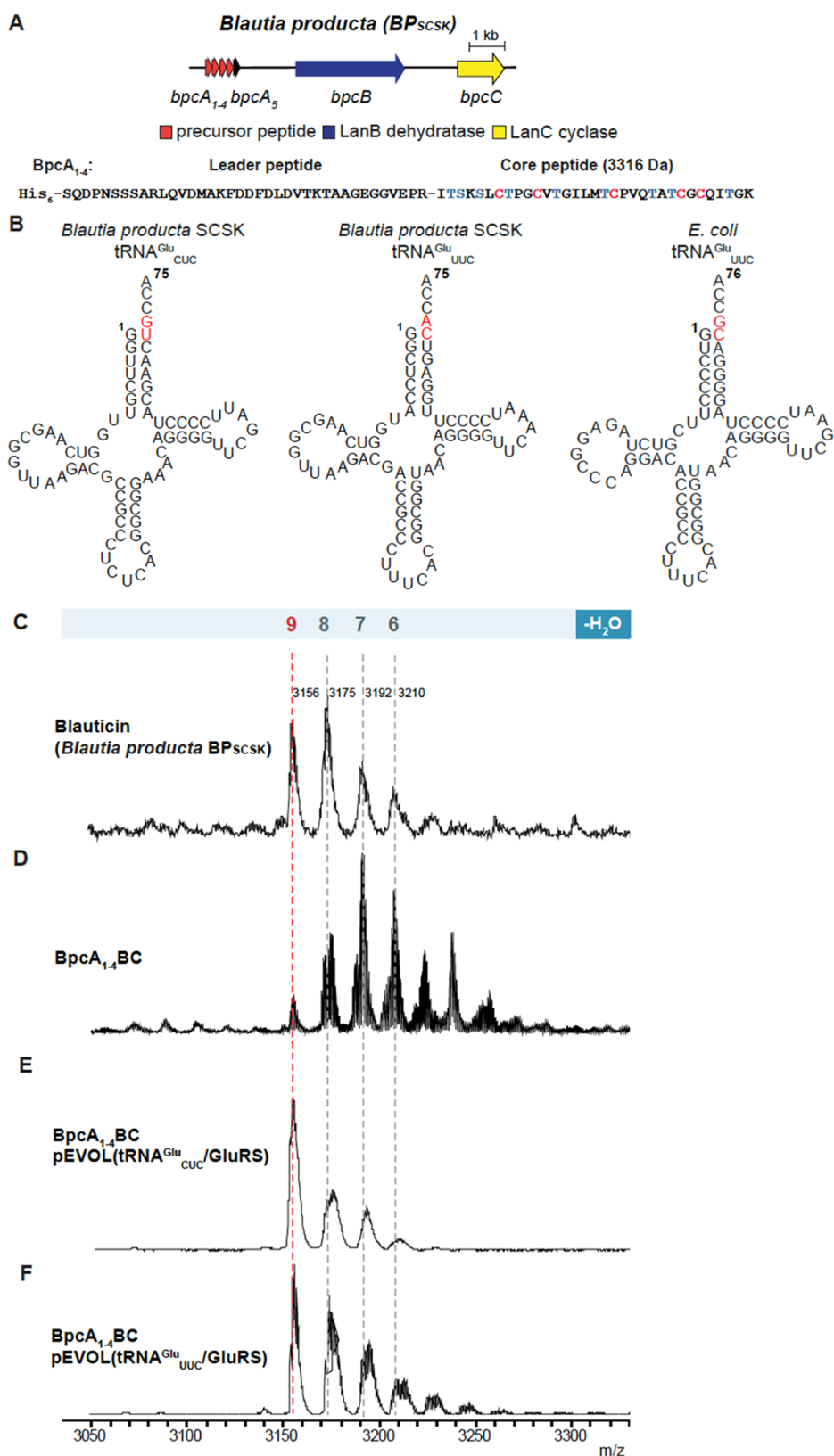


Figure 2. Heterologous production of blauticin using the pEVOL vector in *E. coli* and leader peptide removal with trypsin. (A) Blauticin BGC from *B. producta* SCSK. (B) Predicted cloverleaf structures of *B. producta* SCSK and *E. coli* tRNA^{Glu} made with the tRNAscan-SE algorithm.^{39,40} The proposed major recognition elements of the tRNA^{Glu} acceptor stem used by lantibiotic dehydratases are highlighted in red. (C–F) MALDI-TOF MS analysis of blauticin isolated from BP_{SCSK} (C), His₆-BpcA₁ isolated from the coexpression with BpcBC without (D) and with the pEVOL platform using tRNA^{Glu}_{CUC} (E) or tRNA^{Glu}_{UUC} (F) in *E. coli* after leader peptide removal by trypsin. 6: 6-fold dehydrated BpcA₁ ([M + H]⁺ *m/z* 3210, calcd *m/z* 3208); 7: 7-fold dehydrated BpcA₁ ([M + H]⁺ *m/z* 3192, calcd *m/z* 3190); 8: 8-fold dehydrated BpcA₁ ([M + H]⁺ *m/z* 3175, calcd *m/z* 3172); 9: 9-fold dehydrated BpcA₁ ([M + H]⁺ *m/z* 3156, calcd *m/z* 3154). For high resolution tandem MS data, see Figure S6.

found in mammalian guts. From this approach, we identified 41 unique lanthipeptide candidates (Supporting Information). To find close homologues of nisin and related lantibiotics, we filtered the results based on the following criteria. First, we set a maximum on the peptide length. Because both nisin A and blauticin have 57 residues, including the leader peptide, any length significantly longer than that was unlikely to yield nisin-like lantibiotics. Indeed, WP_117994378.1_29961, a candidate with a length of 71, showed minimal sequence similarity to nisin A (Figure S1). We therefore set the maximum length as 72 residues. Second, the cysteine positions in the peptide needed to align with the ring-forming Cys residues in nisin A and blauticin based on a multiple sequence alignment (Figure S1). We further consolidated sequences that differed only in leader sequences but were the same in the core peptide. Six unique class I lantibiotic sequences, including two known examples, blauticin from *B. producta* and nisin O from *Blautia obeum*,³¹ were identified (Figure 1B, Supporting Information). In fact, the blauticin precursor peptide was also found in *Blautia coccoides* and nisin O was also found within a *Faecalicatena contorta* genome. The sequences of four novel nisin-like class I lantibiotic candidates were compared to the prototypical lantibiotics nisin A and blauticin, as shown in Figure 1B. Lan-Df from *Dorea formicigenerans* was identified to be a close homologue of nisin O, with one amino acid different from nisin O in ring A. Lan-CE02 from *Clostridium* sp. E02 further deviates from the prototype lantibiotics with unique residues spanning across the peptide. We discovered two variants, Lan-P49.1 and Lan-P49.2, from the same genome of *Pseudobutyrvibrio* sp. 49. Lan-P49.1 and Lan-P49.2 both share the same sequences as blauticin in ring A and B at the N termini of the peptides, but the C-termini of the peptides including the hinge region between rings C and D are different from nisin A and blauticin. This hinge region has been shown to be important for pore formation and antimicrobial activity.^{32–35}

Heterologous Expression of Blauticin in *E. coli*. The genome of *B. producta* SCSK has been sequenced, assembled, and annotated.¹⁸ To heterologously express blauticin in *E. coli*, a three-plasmid-based expression platform that was developed previously for other lantibiotics was applied (Figure S2A).¹⁷ In the current version, this platform includes a pETDuet plasmid that encodes a His-tagged blauticin leader and a core sequence. The blauticin leader sequence is recognized by blauticin-specific LanB and LanC (*bpcB* and *bpcC* gene, respectively) encoded in the pCDFDuet plasmid. A third pEVOL plasmid encodes two copies of glutamyl-tRNA synthetase (GluRS) from *B. producta* (one under an inducible promoter araBAD, the other under a constitutive promoter glnS) and a copy of tRNA^{Glu} from *B. producta* under a constitutive promoter proK. The availability of cognate glutamyl-tRNA was envisioned to ensure optimal catalytic activity of BpcB as the sequence of tRNA^{Glu} strongly affects LanB dehydration activity.¹⁵ Coding sequences of *bpcB* and *bpcC* genes were codon-optimized for expression in *E. coli* (Supporting Information). Heterologously expressed lantibiotic precursors were purified from cell lysate by metal affinity chromatography, followed by trypsin digestion for leader peptide removal and RP-HPLC purification (Figure S2B,C).

Among the five BP_{SCSK} lantibiotic precursors that are encoded in the blauticin BGC, the BP_{SCSK} lantibiotic precursors BpcA₁–BpcA₄ are four identical copies of the blauticin precursor peptide and BpcA₅ is a fifth peptide, the

function of which remains to be identified (Figure 2A).¹⁸ An initial attempt of coexpressing His₆-tagged BpcA₁ with BpcB and BpcC in *E. coli* in the absence of the pEVOL plasmid resulted in a mixture of zero to nine dehydrations with the 9-fold dehydrated peptide as one of the least abundant products after leader peptide removal (Figures 2D and S3B). The poor dehydratase activity is likely the result of sequence differences of the major recognition elements for the lantibiotic dehydratases that are located on the acceptor stem of tRNA^{Glu} when comparing *E. coli* and *B. producta* sequences (Figure 2B). After incorporating the pEVOL vector that encodes *B. producta* SCSK GluRS and tRNA^{Glu}_{CUC} in the expression system, up to nine dehydrations were observed by matrix-assisted laser desorption ionization time-of-flight mass spectrometry (MALDI-TOF MS) after trypsin removal of the leader peptide. The mass distribution of the product was similar as that of wild-type blauticin that was isolated from the producing organism (Figures 2C,E and S4A,C). Production of lantibiotics as a mixture of peptides with different dehydration states in the native producing organism is not uncommon and is for example also observed for the commercial food preservative nisin^{36,37} (Figure S6J) or a recently reported lanthipeptide from the human oral microbiome that has pro-immune activity.³⁸ We further purified the blauticin mixture with RP-HPLC and collected its fully dehydrated form (nine dehydrations; Figure S4A) and compared its antimicrobial activity to the dehydration mixture. We observed a similar minimal inhibitory concentration (MIC) of fully dehydrated blauticin, mixed dehydrated blauticin, and native blauticin against vancomycin-resistant *Enterococcus faecium* ATCC700221 (VRE) (Figure S4B).

A previous report studied the tRNA specificity of the lantibiotic dehydratase MibB involved in the biosynthesis of NAI-107 from the Actinobacterium *Microbispora* sp. 107891.¹⁵ MibB was shown to not only discriminate between tRNA^{Glu} from different organisms but to also discriminate between tRNA^{Glu} isoacceptors encoded in the genome of *Microbispora* sp. 107891. A tRNA scanning analysis of the *B. producta* SCSK genome revealed the presence of two tRNA^{Glu} genes encoding tRNA^{Glu}_{CUC} and tRNA^{Glu}_{UUC} isoacceptors (Figure 2B).^{39,40} The presence of the two different tRNA^{Glu} types prompted an investigation into whether the dehydratase BpcB displayed isoacceptor preference. We coexpressed each of the two isoacceptors in the pEVOL vector with BpcA₁, BpcB, and BpcC in *E. coli*. MALDI-TOF MS analysis of dehydration assays revealed that BpcA₁ dehydration was similarly improved when either tRNA^{Glu}_{CUC} or tRNA^{Glu}_{UUC} was used as the isoacceptor, with tRNA^{Glu}_{UUC} perhaps yielding slightly more BpcA with less dehydration compared to tRNA^{Glu}_{CUC} (Figures 2E,F, and S3C,D). These data indicate that both tRNA^{Glu} isoacceptors from BP_{SCSK} can be used by BpcB.

Isolation and Bioactivities of Novel Class I Lantibiotics. After successful demonstration of the expression of blauticin in *E. coli*, we applied a similar approach to express and isolate the novel nisin-like class I lantibiotics discovered in the genomes of mammalian gut microbiota. Rather than using the precursor peptide and biosynthetic enzymes encoded in the producing organisms, we used the His-tagged blauticin leader sequence and fused to its C-terminus the desired lanthipeptide core sequence. The pETDuet plasmid encoding the chimeric substrate was coexpressed with plasmids encoding BpcB, BpcC, and *B. producta* GluRS and tRNA^{Glu}. Such use of one set of producing enzymes for production of structurally closely

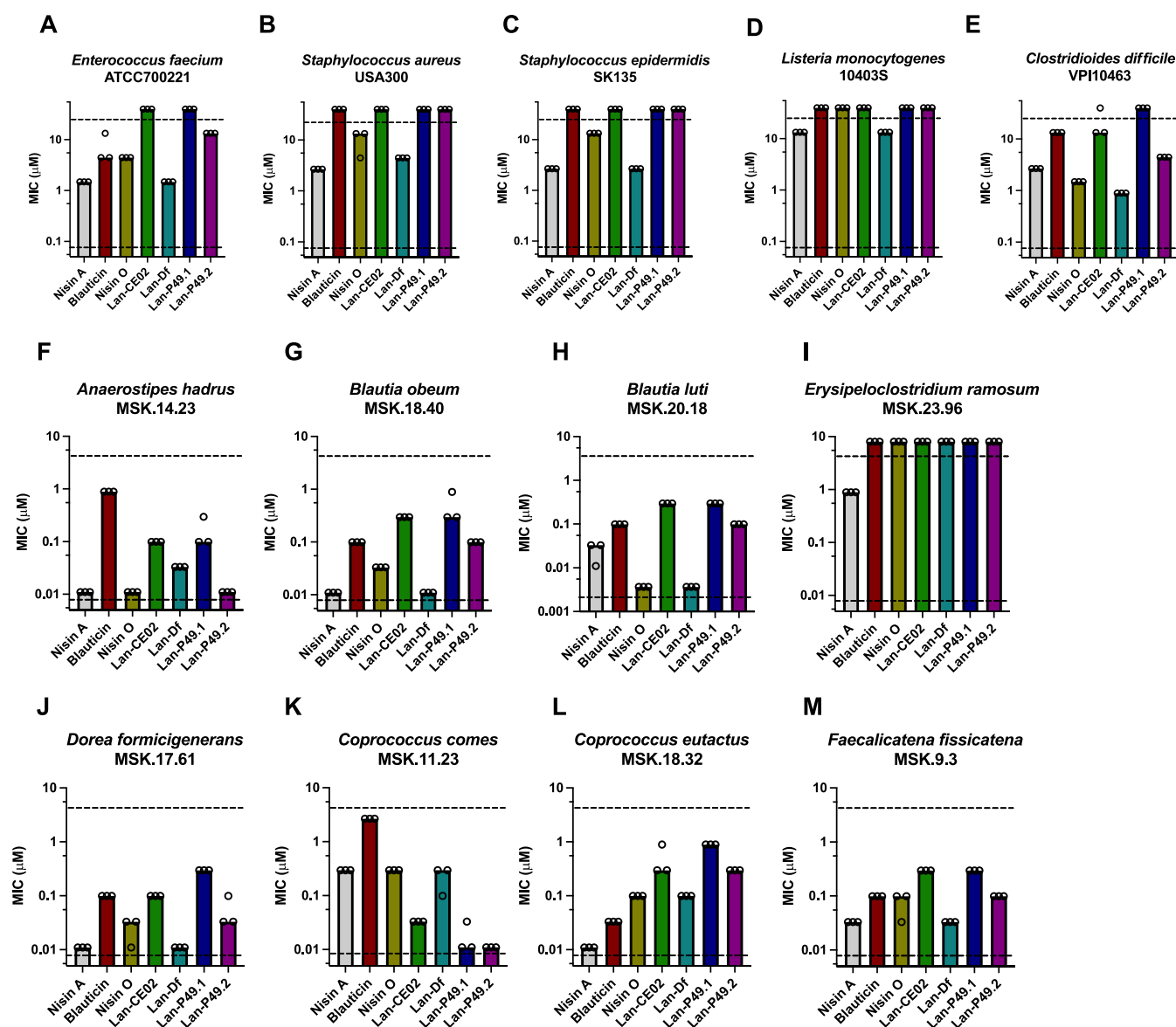


Figure 3. Minimal inhibitory concentration (MIC) of the panel of lantibiotics against human pathogens (A–E) and human gut commensals (F–M). Each dot indicates one measurement of MIC value, determined by the lowest concentration that caused no or significantly less bacterial growth. Each bar indicates median MIC value. Upper and lower dashed lines indicate upper and lower limits of concentration tested, respectively.

related analogs of a certain lantibiotic has been successfully used previously.⁴¹ The modified lantibiotic precursor peptides were purified and digested with trypsin for leader peptide removal. Fully dehydrated Lan-CE02, Lan-Df, Lan-P49.1, and Lan-P49.2 were observed by MALDI-TOF MS (Figure S5 and Table S1). Tandem electrospray ionization (ESI) MS analyses were consistent with these compounds all having the same ring pattern as that of nisin/blauticin (Figure S6). As has been pointed out before,⁴² the number of potential isomers with different ring patterns for these types of peptides is very large (>6500) if cyclization was nonselective, and nonenzymatic cyclization does not provide active nisin.⁴³ Conversely, the LanC cyclases (NisC for nisin and BpcC for this study) govern the site-selectivity of thia-Michael addition to provide a single-ring pattern through a mechanism that is still not understood.

Next, we set out to test the antimicrobial activities of these purified lantibiotics against a panel of Gram-positive bacteria that are representatives of some of the most prevalent human pathogens: VRE, Methicillin-resistant *S. aureus* USA300

(MRSA), Methicillin-resistant *Staphylococcus epidermidis* SK135 (MRSE), *Listeria monocytogenes* 10403S, and *Clostridioides difficile* VPI10463. We examined the growth of bacteria in a 96-well plate under a concentration gradient of lantibiotics under anaerobic conditions (Figure S2B). In general, nisin A and Lan-Df had the strongest inhibitory activities against pathogens based on their MIC, followed by nisin O. Blausicin, Lan-CE02, and Lan-P49.2 had intermediate activities, while Lan-P49.1 had the weakest activity (Figure 3A–E). Comparing across the pathogen panel, VRE, and *C. difficile* were more sensitive to lantibiotic treatment, while *L. monocytogenes* was the most resistant among the panel tested.

Antibiotic treatment may result in collateral damage to commensal bacteria in the human microbiome, leading to dysbiosis and susceptibility to various diseases.⁴⁴ How lantibiotics impact Gram-positive commensals from the human gut has remained unclear. Therefore, we performed antimicrobial activity tests of these lantibiotics against selected Gram-positive human gut commensals, most of which belong

Table 1. Number of Genes in Pathogens Related to Resistance to Class I Lantibiotics

| bacterial strain | <i>C. difficile</i> VPI10463 | <i>E. faecium</i> ATCC700221 | <i>S. aureus</i> USA300 | <i>S. epidermidis</i> SK135 | <i>L. monocytogenes</i> 10403s | mechanism of resistance |
|-------------------------|---------------------------------|---------------------------------|----------------------------|--------------------------------|-----------------------------------|-------------------------------|
| nisin A MIC (μ M) | 2.67 | 1.48 | 2.67 | 2.67 | 2.67 | |
| median MIC (μ M) | 4.44 | 13.3 | >13.3 | >13.3 | >13.3 | |
| cell wall biosynthesis | | | | | | |
| complete <i>dltABCD</i> | 1 | 1 | 1 | 1 | 1 | changing cell wall charge |
| efflux pump | | | | | | |
| complete <i>lanFEG</i> | 1 | 0 | 1 | 0 | 0 | lantibiotic efflux |
| complete <i>bceAB</i> | 0 | 1 | 1 | 1 | 1 | bacitracin efflux |
| others | | | | | | |
| <i>telA</i> | 1 | 1 | 1 | 1 | 1 | unknown |
| <i>mprF</i> | 0 | 2 | 1 | 1 | 1 | changing cell membrane charge |
| <i>nsr</i> | 0 | 0 | 0 | 0 | 0 | lantibiotic protease |
| <i>lanI</i> | 0 | 0 | 0 | 0 | 0 | lantibiotic sequestration |

Table 2. Number of Genes in Human Gut Commensals Related to Resistance of Nisin-like Lantibiotics

| bacterial strain | <i>A. hadrus</i> MSK.14.23 | <i>D. formicigenerans</i> MSK.17.61 | <i>B. obeum</i> MSK.18.40 | <i>Coprococcus eutactus</i> MSK.18.32 | <i>B. luti</i> MSK.20.18 | <i>F. fissicatena</i> MSK.9.3 | <i>C. comes</i> MSK.11.23 | <i>E. ramosum</i> MSK.23.96 | mechanism of resistance |
|-------------------------|-------------------------------|--|------------------------------|--|-----------------------------|----------------------------------|------------------------------|--------------------------------|-------------------------------|
| nisin A MIC (μ M) | 0.0110 | 0.0110 | 0.0110 | 0.0110 | 0.0329 | 0.0329 | 0.296 | 0.889 | |
| median MIC (μ M) | 0.0329 | 0.0329 | 0.0988 | 0.0988 | 0.0988 | 0.0988 | 0.296 | >2.67 | |
| cell wall biosynthesis | | | | | | | | | |
| complete <i>dltABCD</i> | 0 | 0 | 0 | 0 | 0 | 0 | 0 | 0 | changing cell wall charge |
| efflux pump | | | | | | | | | |
| complete <i>lanFEG</i> | 0 | 0 | 0 | 0 | 0 | 0 | 0 | 0 | lantibiotic efflux |
| complete <i>bceAB</i> | 1 | 0 | 0 | 1 | 0 | 0 | 1 | 2 | bacitracin efflux |
| others | | | | | | | | | |
| <i>telA</i> | 0 | 0 | 1 | 0 | 1 | 1 | 1 | 0 | unknown |
| <i>mprF</i> | 0 | 0 | 0 | 0 | 0 | 0 | 0 | 0 | changing cell membrane charge |
| <i>nsr</i> | 0 | 0 | 0 | 0 | 0 | 0 | 0 | 0 | lantibiotic protease |
| <i>lanI</i> | 0 | 0 | 0 | 0 | 0 | 0 | 0 | 0 | lantibiotic sequestration |

to the Lachnospiraceae family, one of the most abundant bacterial families in the human gut.²⁷ In general, human gut commensals were more susceptible to the set of investigated lantibiotics compared to pathogens (Figure 3). The activities of the lantibiotics tested generally followed the trend of those against Gram-positive pathogens; while nisin A and Lan-Df were generally more effective in growth inhibition, Lan-P49.1, Lan-P49.2, and Lan-CE02 had weaker antimicrobial activities (Figure 3F–M). Among all, *Erysipeloclostridium ramosum* MSK.23.96 displayed the highest resistance to lantibiotics compared to other commensals tested. Interestingly, *Coprococcus comes* MSK.11.23 had an opposite sensitivity profile; it was relatively resistant to nisin A, nisin O, and Lan-Df, while it was more sensitive to Lan-P49.1 and LanP49.2.

To further investigate the mechanisms of action of these nisin-like lantibiotics, we performed liposome permeabilization assays using liposomes with or without lipid II (Figure S7). We observed that the fraction of liposomes containing lipid II that were permeabilized upon incubation with lantibiotics largely correlated with their MIC values against bacteria: nisin O, Lan-Df, and Lan-P49.2, as well as blauticin and nisin A, strongly

induced permeabilization of lipid II-containing liposomes, while Lan-CE02 and Lan-P49.1 were not as effective (Figure S7B). We further tested the most active lantibiotics for their permeabilization activities on liposomes without lipid II. Nisin O, Lan-Df, and Lan-P49.2, as well as blauticin and nisin A, had decreased permeabilization activities on liposomes without lipid II compared to liposomes with lipid II (Figure S7). These findings suggest that the mechanism of action of these nisin-like lantibiotics is mainly lipid II-dependent membrane permeabilization, but they also disrupt membranes less potently in the absence of lipid II in a nonspecific mechanism. Unexpectedly, blauticin in the mixed dehydration state had decreased permeabilization activity compared to fully dehydrated blauticin (Figure S7B), even though the MIC values against VRE were similar (Figure S4B).

Lantibiotic Resistance Genes in Pathogens and Commensals. The differences in lantibiotic susceptibility profiles of pathogens and human gut commensals led to further investigation of potential lantibiotic resistance mechanisms encoded in the genomes of gut bacteria. Many mechanisms of lantibiotic resistance in bacteria have been reported, mostly

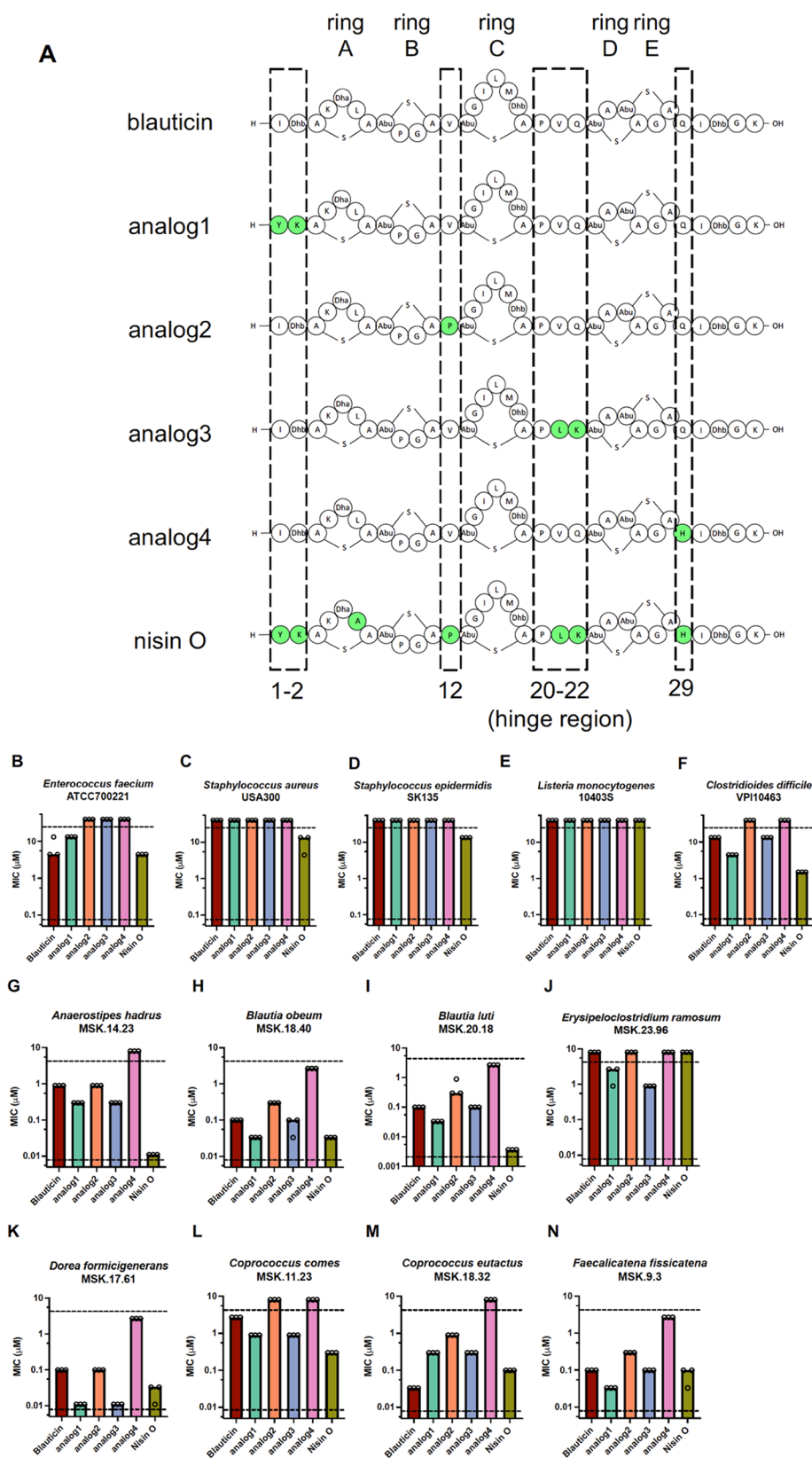


Figure 4. Structure–activity relationship (SAR) study of blauticin and comparison with Nisin O. (A) Illustration of blauticin, SAR analogs, and nisin O. Dashed boxes indicate regions from nisin O swapped into the blauticin backbone individually that created each SAR analog. Green shading indicates residues different from blauticin. Five rings in the structure are denoted on the top. Residue numbers and hinge region are denoted at the bottom. (B–N) Minimal inhibitory concentration (MIC) of the lantibiotic analogs against human pathogens (B–F) and human gut commensals (G–N). Each dot indicates one measurement of MIC value, determined by the lowest concentration that caused no or significantly less bacterial growth. Each bar indicates median MIC value. Upper and lower dashed lines indicate the upper and lower limits of concentration tested, respectively. Observed and expected masses for each compound are listed in Table S1.

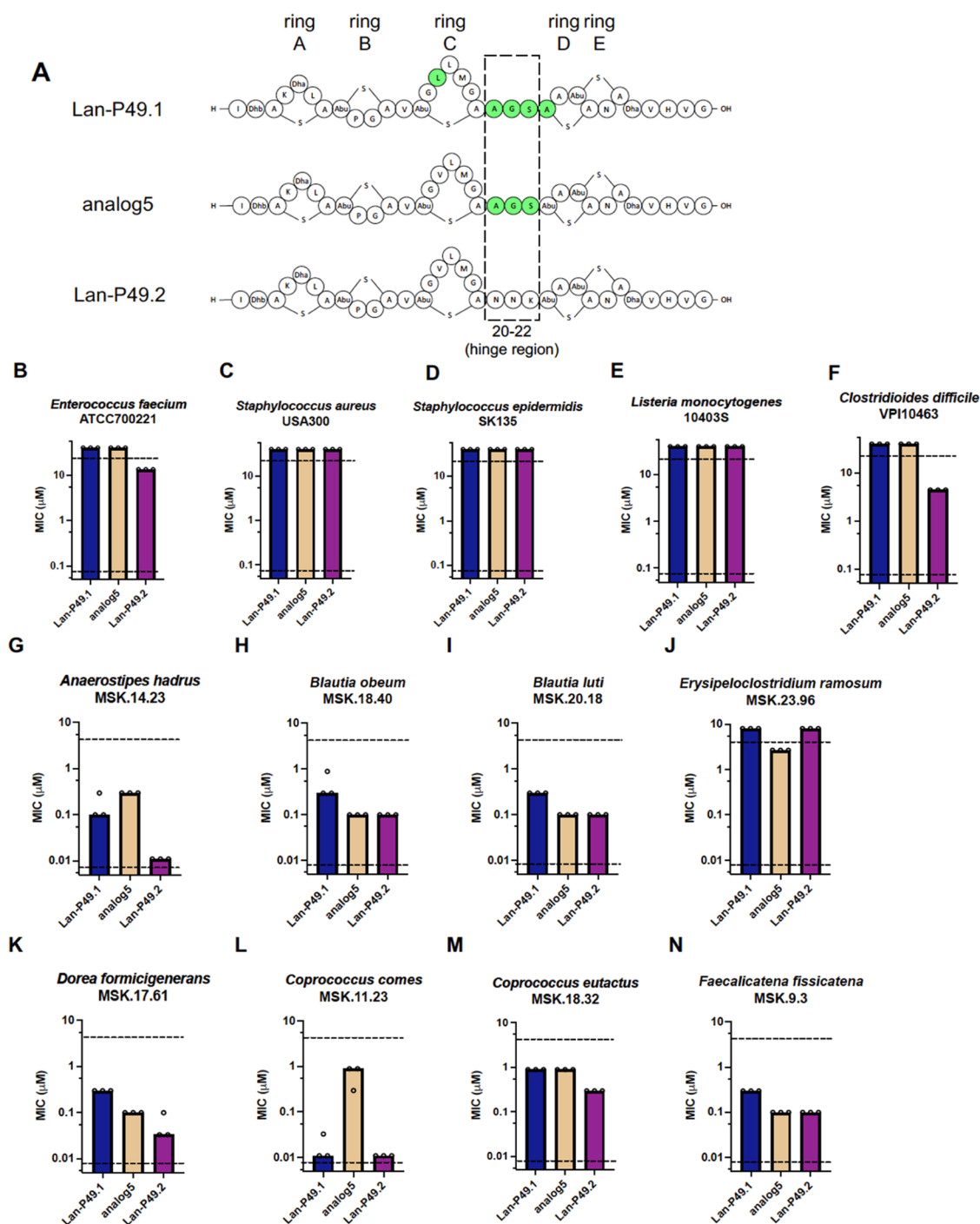


Figure 5. Structure–activity relationship (SAR) study of Lan-P49.1 versus Lan-P49.2. (A) Illustration of Lan-P49.1, analog5, and Lan-P49.2. The dashed box indicates the hinge region from Lan-P49.1 swapped into the Lan-P49.2 backbone that created analog5. Green shading indicates residues different from P49.2. Five rings in the structure are denoted on the top. Residue numbers and hinge region are denoted at the bottom. (B–N) Minimal inhibitory concentration (MIC) of the lantibiotic analogs against human pathogens (B–F) and human gut commensals (G–N). Each dot indicates one measurement of MIC value, determined by the lowest concentration that caused no or significantly less bacterial growth. Each bar indicates median MIC value. Upper and lower dashed lines indicate upper and lower limits of concentration tested, respectively. Observed and expected masses for each compound are listed in Table S1.

revealed through genetic screening of pathogens. One major resistance mechanism is bacterial cell wall modifications. The *dltABCD* operon is responsible for the D-alanylation of lipoteichoic acids (LTA) and wall teichoic acids (WTA), resulting in an increase of positive charges in the cell wall and the repulsion of cationic lantibiotics.^{45,46} Another major resistance mechanism is efflux pumps. The LanFEG three-

component transporter and homologues can expel lantibiotics,^{30,47,48} while the BceAB two-component transporter, originally reported as a bacitracin efflux pump, also provides cross-protection against lantibiotics.⁴⁹ Other resistance mechanisms include the tellurite resistance gene *telA*,⁵⁰ cell membrane modifications by *mprF*,⁵¹ the nisin resistance protein NSR,^{52,53} and lantibiotic self-resistance proteins

LanI.⁵⁴ Of these, LanFEG and LanI are often found in lantibiotic BGCs.

We performed a Hidden Markov Model and BLAST search for the aforementioned genes among the genomes of pathogens and human gut commensals tested. For resistance mechanisms that require multiple genes (*dltABCD*, *bceAB*, and *lanFEG*), only the complete presence as an operon was counted. The numbers of corresponding genes in each genome are listed in Tables 1 and 2. Bacteria are listed in ascending order from left to right according to the median MIC value across the nisin-like lantibiotic panel. We found that for most organisms, the numbers of potential resistance-inducing genes present in a specific genome did not correlate with stronger lantibiotic resistance (lower susceptibility). *bceAB* and *mprF* may correlate with resistance in some cases, as the most sensitive *Clostridioides difficile* does not possess these genes. Among human gut commensals, the most resistant *E. ramosum* has more *bceAB* genes than others. However, one of the most sensitive strains, *Anaerostipes hadrus* MSK.14.23, also contains the *bceAB* genes. In conclusion, the numbers of putative resistance genes in these pathogens and commensals cannot fully explain their relative susceptibility to the lantibiotics tested.

Structure–Activity Relationship Studies. Given the high similarity of sequences among the nisin-like lantibiotics encoded in the gut microbiome, we next set out to study the structure–activity relationships (SAR) between specific residues and the antimicrobial activity. Blauticin and nisin O are two lantibiotics derived from *Blautia* species, but their activities vary against both pathogens and commensals, with nisin O being more effective in most cases. Four major regions differ between them: residues 1 and 2 at their N termini, residue 12 between rings B and C, residues 20–22 at the hinge region, and residue 29 at the C termini (Figure 4A). To assess the impact of these individual regions on the antimicrobial activity, we synthesized four blauticin analogs by replacing the blauticin residues with the corresponding residues in nisin O (analog1–analog4) using the expression platform described above (Figures 4A and S8, and Table S1).

The bioactivities of the four analogs were tested against the aforementioned panel of pathogens and gut commensals. In the pathogen panel, analog1 had intermediate antimicrobial activity between blauticin and nisin O, except in the case against VRE (Figure 4B–F), while analog2 to analog4 displayed comparable or reduced activities compared to the two parent lantibiotics. On the other hand, for the gut commensal panel, analog1 and analog3 had intermediate inhibitory activities between blauticin and nisin O for some commensals (Figure 4G–I,L), and had even better antimicrobial activities when targeting *E. ramosum* (Figure 4J) or *D. formicigenerans* (Figure 4K). On the contrary, analogs2 and 4 exhibited diminished activities compared to both parent molecules (Figure 4G–N). Interestingly, for *C. eutactus*, none of the analogs displayed better inhibition than either parent lantibiotic, and it was also the only case when blauticin had a lower MIC than nisin O. These data suggest that the first two residues and the hinge region of nisin-like lantibiotics have a more direct impact on the antimicrobial activity of nisin-like lantibiotics, while single-residue mutations V12P and Q29H had a deleterious impact on antimicrobial activity depending on the context of the backbone.

We further performed SAR studies on two highly similar lantibiotics, Lan-P49.1 and Lan-P49.2. They originate from the

same *Pseudobutyrvibrio* genome, and their amino acid sequences have the largest difference in the hinge region. To test the impact of the hinge region, we swapped the hinge region of Lan-P49.1 into the Lan-P49.2 backbone, creating analog5 (Figures SA and S8, and Table S1). Analog5 had decreased antimicrobial activity against the pathogen panel compared with Lan-P49.2 (Figure SB–F). When tested against the gut commensal panel, analog5 displayed intermediate activity compared to Lan-P49.1 and Lan-P49.2 in most cases (Figure SH,I,K,M,N), reaching the same MIC as that of Lan-P49.1 in some bacteria (Figure SM) and the same MIC as that of Lan-P49.2 in other commensals (Figure SH,I,N). Interestingly, for *A. hadrus* and *C. comes*, analog5 had decreased antimicrobial activity compared to both parent lantibiotics, whereas for *E. ramosum*, analog5 had increased antimicrobial activity. These data demonstrate the importance of the hinge region in determining the antimicrobial activity of nisin-like lantibiotics, and are consistent with an emerging realization that lantibiotics may act differently based on the target organism investigated.⁵⁵

DISCUSSION

Nisin is a class I lantibiotic that has been widely used in the food industry for decades and has been explored as an antimicrobial therapeutic.^{23,26} Nisin A is produced by *L. lactis*, found in milk. However, how nisin and nisin-like lantibiotics might impact the human gut microbiome has not been elucidated, nor has the presence of nisin-like compounds in the human gut microbiome been investigated in detail. The recent discovery of blauticin and nisin analogs clearly indicates that nisin-like molecules are encoded in the human microbiome,^{18,31,56,57} with other analogs detected in the microbiome of other mammals.^{58,59} To first explore the biosynthetic potential of the gut microbiome for lantibiotic production, we systematically performed bioinformatic mining with RODEO for nisin-like lantibiotics derived from gut bacterial genomes. Subsequent filtering, multiple sequence alignment, and manual curation discovered six gut-derived nisin-like lantibiotics, four of which were not reported previously. Our work greatly expands the repertoire of naturally encoded nisin-like lantibiotics from the human gut.

Utilizing an improved heterologous expression platform for lantibiotics in *E. coli*, we produced all six gut-derived lantibiotics in mixed dehydration states. Blauticin is produced in very similar mixed dehydration states by its native host *B. producta*, and its fully dehydrated form has a similar efficacy against VRE compared to its mixture of different dehydration states. This finding, along with the observation that nisin is also produced in various dehydration states in its native producer (e.g., see Figure S6J for commercial nisin A),^{36,37} suggests that nisin-like lantibiotics do not require full dehydration for their antimicrobial activity. Therefore, we used purified lantibiotics in mixed dehydration states in this study because they best represent the naturally produced compounds. Despite similar MIC values, blauticin in mixed dehydration states displayed decreased lipid II-containing liposome permeabilization activity compared with fully dehydrated blauticin. One possible explanation for this finding is that blauticin binding to lipid II without pore formation (e.g., lipid II sequestration⁶⁰) may contribute to killing bacteria.

Gram-positive pathogens and human gut commensals have varied susceptibility profiles toward the panel of lantibiotics tested. Many mechanisms of lantibiotic resistance have been

described in bacteria; besides mechanisms already discussed, an array of two-component systems and cell membrane modification genes have also been reported to confer lantibiotic resistance (see detailed discussion in ref 30). Besides the presence and number of resistance genes in the genome, the regulation and expression of these genes are also important in lantibiotic resistance. While we did not find strong correlations between the numbers of resistance genes and the MICs of the lantibiotic panel tested, future studies of expression and regulation of various resistance genes in bacteria, especially in human gut commensals, will be needed to elucidate the apparent differences in susceptibility among Gram-positive bacteria. Alternatively, other differences between the tested bacteria, such as membrane composition, may account for the different susceptibilities.

To further understand the contribution of specific residues in naturally occurring nisin-like lantibiotics to their antimicrobial activity, we studied the SAR of two pairs of closely related lantibiotics: blauticin versus nisin O, and Lan-P49.1 versus Lan-P49.2. Both SARs revealed that the hinge region is critical in determining the efficacy of these lantibiotics, consistent with previous reports.^{32–35,61} SAR studies of blauticin versus nisin O also found the first two residues to be important for activity. Surprisingly, when residues in blauticin were changed to their counterparts in nisin O (analog2 and analog4), it caused deleterious effects on the antimicrobial activity even against bacteria toward which nisin O has stronger activity than blauticin. Our data suggest that the impact of certain individual residues is context-dependent, implicating intricate interactions among residues along the full length of nisin-like lantibiotics. The 1:1 structure of nisin bound to lipid II has been determined by NMR spectroscopy in DMSO,⁶² and solid-state NMR studies of the lipid II-nisin complex in a membrane environment show that the hinge region is facing the lumen of the pore in the complex.⁶³ However, the details of the structure of the 2:1 nisin to lipid II complex that is believed to be present in the pores that are made up of eight nisin and four lipid II molecules³⁴ is currently still not known. Our results showing high sensitivity to replacing even single residues suggest that it may be that the naturally occurring sequences of nisin-like lantibiotics may have evolved such that covariance of residues is important for forming the 2:1 ratio structure and/or that the residues facing the lumen of the pore in the complex are important for bioactivity.

In summary, we have discovered gut-derived novel class I lantibiotics through bioinformatic mining, produced them using an improved heterologous expression platform, and studied their antimicrobial activities against both pathogens and human gut commensals. These characterizations and subsequent SAR studies have revealed the antimicrobial spectrum of both pathogens and human gut commensals, providing insights that will be valuable for the future development of lantibiotic-based therapeutics and food preservatives.

■ ASSOCIATED CONTENT

SI Supporting Information

The Supporting Information is available free of charge at <https://pubs.acs.org/doi/10.1021/acschembio.3c00577>.

Experimental procedures; bioinformatic analysis and MSA (Figure S1); improved expression platform and lantibiotic production workflow (Figure S2); MALDI-

TOF MS analysis (Figures S3, S5, and S8); bioactivities of blauticin (Figure S4); tandem MS analysis (Figure S6); liposome permeabilization assays (Figure S7); lantipeptide expected and observed masses (Table S1); oligonucleotides and gene fragments used in this study (Table S2); and bacterial genomes and PFAM HMM used in this study (Table S3); materials and methods, Figures S1–S8; Tables S1–S3 (PDF)

■ AUTHOR INFORMATION

Corresponding Authors

Zhenrun J. Zhang – Duchossois Family Institute, University of Chicago, Chicago, Illinois 60637, United States; Department of Microbiology, University of Chicago, Chicago, Illinois 60637, United States; orcid.org/0000-0002-2124-5539; Email: zjzhang@bsd.uchicago.edu

Eric G. Pamer – Duchossois Family Institute, University of Chicago, Chicago, Illinois 60637, United States; Departments of Medicine and Pathology, University of Chicago, Chicago, Illinois 60637, United States; Email: egpamer@bsd.uchicago.edu

Wilfred A. van der Donk – Department of Biochemistry, University of Illinois at Urbana—Champaign, Urbana, Illinois 61801, United States; Department of Chemistry, The Howard Hughes Medical Institute, University of Illinois at Urbana—Champaign, Urbana, Illinois 61801, United States; orcid.org/0000-0002-5467-7071; Email: vddonk@illinois.edu

Authors

Chunyu Wu – Department of Biochemistry, University of Illinois at Urbana—Champaign, Urbana, Illinois 61801, United States; orcid.org/0000-0002-0312-3247

Ryan Moreira – Department of Chemistry, The Howard Hughes Medical Institute, University of Illinois at Urbana—Champaign, Urbana, Illinois 61801, United States; orcid.org/0000-0003-0694-219X

Darian Dorantes – Department of Biochemistry, University of Illinois at Urbana—Champaign, Urbana, Illinois 61801, United States

Téa Pappas – Duchossois Family Institute, University of Chicago, Chicago, Illinois 60637, United States

Anitha Sundararajan – Duchossois Family Institute, University of Chicago, Chicago, Illinois 60637, United States

Huaiying Lin – Duchossois Family Institute, University of Chicago, Chicago, Illinois 60637, United States

Complete contact information is available at:

<https://pubs.acs.org/doi/10.1021/acschembio.3c00577>

Author Contributions

#Z.J.Z. and C.W. contributed equally to this study.

Funding

Z.J.Z. was supported by The GI Research Foundation early career grant, and R.M. was supported by a fellowship from the Life Science Research Foundation funded by HHMI. This work was supported by US National Institutes of Health grants R01AI095706, P01 CA023766, U01 AI124275, and R01 AI042135 to E.G.P., and by the Duchossois Family Institute of the University of Chicago. W.A.V. is an Investigator of the Howard Hughes Medical Institute. The Bruker UltrafleXtreme MALDI TOF/TOF mass spectrometer used for this work was purchased in part with a grant from the National Center for

Research Resources, National Institutes of Health (S10 RR027109 A).

Notes

The authors declare the following competing financial interest(s): E.G.P. serves on the advisory board of Diversigen; is an inventor on patent applications WPO2015179437A1, titled Methods and compositions for reducing *Clostridium difficile* infection, and WO2017091753A1, titled Methods and compositions for reducing vancomycin-resistant enterococci infection or colonization; and receives royalties from Seres Therapeutics, Inc. The other authors are not aware of any affiliations, memberships, funding, or financial holdings that might be perceived as affecting the objectivity of this manuscript.

ACKNOWLEDGMENTS

The authors thank members of the E.G.P. laboratory who have provided valuable feedback on this manuscript. This study is subject to HHMI's Open Access to Publications policy. HHMI laboratory heads have previously granted a nonexclusive CC BY 4.0 license to the public and a sublicensable license to HHMI in their research articles. Pursuant to those licenses, the author-accepted manuscript of this article can be made freely available under a CC BY 4.0 license immediately upon publication.

REFERENCES

- (1) Heilbronner, S.; Krismer, B.; Brötz-Oesterhelt, H.; Peschel, A. The microbiome-shaping roles of bacteriocins. *Nat. Rev. Microbiol.* **2021**, *19*, 726–739.
- (2) Verma, A.; Banerjee, R.; Dwivedi, H. P.; Juneja, V. K. *Encyclopedia of Food Microbiology*, 2nd ed.; Batt, C. A.; Tortorello, M. L., Eds.; Academic Press, 2014; Vol. 3.
- (3) Deisinger, J. P.; Arts, M.; Kotsogianni, I.; Puls, J. S.; Grein, F.; Ortiz-López, F. J.; Martin, N. I.; Müller, A.; Genilloud, O.; Schneider, T. Dual targeting of the class V lanthipeptide antibiotic cacoindin. *iScience* **2023**, *26*, No. 106394.
- (4) Tracanna, V.; de Jong, A.; Medema, M. H.; Kuipers, O. P. Mining prokaryotes for antimicrobial compounds: from diversity to function. *FEMS Microbiol. Rev.* **2017**, *41*, 417–429.
- (5) Ongpipattanakul, C.; Desormeaux, E. K.; DiCaprio, A.; van der Donk, W. A.; Mitchell, D. A.; Nair, S. K. Mechanism of action of ribosomally synthesized and post-translationally modified peptides. *Chem. Rev.* **2022**, *122*, 14722–14814.
- (6) Arnison, P. G.; Bibb, M. J.; Bierbaum, G.; Bowers, A. A.; Bugni, T. S.; Bulaj, G.; Camarero, J. A.; Campopiano, D. J.; Challis, G. L.; Clardy, J.; Cotter, P. D.; Craik, D. J.; Dawson, M.; Dittmann, E.; Donadio, S.; Dorrestein, P. C.; Entian, K. D.; Fischbach, M. A.; Garavelli, J. S.; Göransson, U.; Gruber, C. W.; Haft, D. H.; Hemscheidt, T. K.; Hertweck, C.; Hill, C.; Horswill, A. R.; Jaspars, M.; Kelly, W. L.; Klinman, J. P.; Kuipers, O. P.; Link, A. J.; Liu, W.; Marahiel, M. A.; Mitchell, D. A.; Moll, G. N.; Moore, B. S.; Müller, R.; Nair, S. K.; Nes, I. F.; Norris, G. E.; Olivera, B. M.; Onaka, H.; Patchett, M. L.; Piel, J.; Reaney, M. J.; Rebuffat, S.; Ross, R. P.; Sahl, H. G.; Schmidt, E. W.; Selsted, M. E.; Severinov, K.; Shen, B.; Sivonen, K.; Smith, L.; Stein, T.; Süßmuth, R. D.; Tagg, J. R.; Tang, G. L.; Truman, A. W.; Vederas, J. C.; Walsh, C. T.; Walton, J. D.; Wenzel, S. C.; Willey, J. M.; van der Donk, W. A. Ribosomally synthesized and post-translationally modified peptide natural products: overview and recommendations for a universal nomenclature. *Nat. Prod. Rep.* **2013**, *30*, 108–160.
- (7) Montalbán-López, M.; Scott, T. A.; Ramesh, S.; Rahman, I. R.; van Heel, A. J.; Viel, J. H.; Bandarian, V.; Dittmann, E.; Genilloud, O.; Goto, Y.; Grande Burgos, M. J.; Hill, C.; Kim, S.; Koehnke, J.; Latham, J. A.; Link, A. J.; Martínez, B.; Nair, S. K.; Nicolet, Y.; Rebuffat, S.; Sahl, H.-G.; Sareen, D.; Schmidt, E. W.; Schmitt, L.; Severinov, K.; Süßmuth, R. D.; Truman, A. W.; Wang, H.; Weng, J.-K.; van Wezel, G. P.; Zhang, Q.; Zhong, J.; Piel, J.; Mitchell, D. A.; Kuipers, O. P.; van der Donk, W. A. New developments in RiPP discovery, enzymology and engineering. *Nat. Prod. Rep.* **2021**, *38*, 130–239.
- (8) Eslami, S. M.; van der Donk, W. A. Proteases involved in leader peptide removal during RiPP biosynthesis. *ACS Bio. Med. Chem. Au* **2024**, DOI: 10.1021/acsbiomedchemau.3c00059.
- (9) Russell, A. H.; Truman, A. W. Genome mining strategies for ribosomally synthesized and post-translationally modified peptides. *Comput. Struct. Biotechnol. J.* **2020**, *18*, 1838–1851.
- (10) Zhong, Z.; He, B.; Li, J.; Li, Y. X. Challenges and advances in genome mining of ribosomally synthesized and post-translationally modified peptides (RiPPs). *Synth. Syst. Biotechnol.* **2020**, *5*, 155–172.
- (11) Repka, L. M.; Chekan, J. R.; Nair, S. K.; van der Donk, W. A. Mechanistic understanding of lanthipeptide biosynthetic enzymes. *Chem. Rev.* **2017**, *117*, 5457–5520.
- (12) Tietz, J. I.; Schwalen, C. J.; Patel, P. S.; Maxson, T.; Blair, P. M.; Tai, H. C.; Zakai, U. I.; Mitchell, D. A. A new genome-mining tool redefines the lasso peptide biosynthetic landscape. *Nat. Chem. Biol.* **2017**, *13*, 470–478.
- (13) Walker, M. C.; Eslami, S. M.; Hetrick, K. J.; Ackenhusen, S. E.; Mitchell, D. A.; van der Donk, W. A. Precursor peptide-targeted mining of more than one hundred thousand genomes expands the lanthipeptide natural product family. *BMC Genomics* **2020**, *21*, 387.
- (14) Ortega, M. A.; Hao, Y.; Zhang, Q.; Walker, M. C.; van der Donk, W. A.; Nair, S. K. Structure and mechanism of the tRNA-dependent lantibiotic dehydratase NisB. *Nature* **2015**, *517*, 509–512.
- (15) Ortega, M. A.; Hao, Y.; Walker, M. C.; Donadio, S.; Sosio, M.; Nair, S. K.; van der Donk, W. A. Structure and tRNA specificity of MibB, a lantibiotic dehydratase from Actinobacteria involved in NAI-107 biosynthesis. *Cell Chem. Biol.* **2016**, *23*, 370–380.
- (16) Bothwell, I. R.; Caetano, T.; Sargsian, R.; Mendo, S.; van der Donk, W. A. Structural analysis of class I lanthipeptides from *Pedobacter lusitanus* NL19 reveals an unusual ring pattern. *ACS Chem. Biol.* **2021**, *16*, 1019–1029.
- (17) Lee, H.; Wu, C.; Desormeaux, E. K.; Sargsian, R.; van der Donk, W. A. Improved production of class I lanthipeptides in *Escherichia coli*. *Chem. Sci.* **2023**, *14*, 2537–2546.
- (18) Kim, S. G.; Becattini, S.; Moody, T. U.; Shliaha, P. V.; Littmann, E. R.; Seok, R.; Gjonbalaj, M.; Eaton, V.; Fontana, E.; Amoretti, L.; Wright, R.; Caballero, S.; Wang, Z. M. X.; Jung, H. J.; Morjaria, S. M.; Leiner, I. M.; Qin, W.; Ramos, R. J. J. F.; Cross, J. R.; Narushima, S.; Honda, K.; Peled, J. U.; Hendrickson, R. C.; Taur, Y.; van den Brink, M. R. M.; Pamer, E. G. Microbiota-derived lantibiotic restores resistance against vancomycin-resistant *Enterococcus*. *Nature* **2019**, *572*, 665–669.
- (19) Breukink, E.; Wiedemann, I.; van Kraaij, C.; Kuipers, O. P.; Sahl, H. G.; de Kruijff, B. Use of the cell wall precursor lipid II by a pore-forming peptide antibiotic. *Science* **1999**, *286*, 2361–2364.
- (20) Breukink, E.; de Kruijff, B. Lipid II as a target for antibiotics. *Nat. Rev. Drug Discovery* **2006**, *5*, 321–332.
- (21) Bierbaum, G.; Sahl, H. G. Lantibiotics: mode of action, biosynthesis and bioengineering. *Curr. Pharm. Biotechnol.* **2009**, *10*, 2–18.
- (22) Breukink, E.; van Heusden, H. E.; Vollmerhaus, P. J.; Swiezewska, E.; Brunner, L.; Walker, S.; Heck, A. J.; de Kruijff, B. Lipid II is an intrinsic component of the pore induced by nisin in bacterial membranes. *J. Biol. Chem.* **2003**, *278*, 19898–19903, DOI: 10.1074/jbc.M301463200.
- (23) Lubelski, J.; Rink, R.; Khusainov, R.; Moll, G. N.; Kuipers, O. P. Biosynthesis, immunity, regulation, mode of action and engineering of the model lantibiotic nisin. *Cell. Mol. Life Sci.* **2008**, *65*, 455–476.
- (24) Ross, A. C.; Vederas, J. C. Fundamental functionality: recent developments in understanding the structure-activity relationships of lantibiotic peptides. *J. Antibiot.* **2011**, *64*, 27–34.
- (25) Field, D.; Fernandez de Ullivarri, M.; Ross, R. P.; Hill, C. After a century of nisin research - where are we now? *FEMS Microbiol. Rev.* **2023**, *47*, No. fuad023.

- (26) Delves-Broughton, J.; Blackburn, P.; Evans, R. J.; Hugenholtz, J. Applications of the bacteriocin, nisin. *Antonie van Leeuwenhoek* **1996**, *69*, 193–202.
- (27) Sorbara, M. T.; Littmann, E. R.; Fontana, E.; Moody, T. U.; Kohout, C. E.; Gjonbalaj, M.; Eaton, V.; Seok, R.; Leiner, I. M.; Pamer, E. G. Functional and genomic variation between human-derived isolates of *Lachnospiraceae* reveals inter- and intra-species diversity. *Cell Host Microbe* **2020**, *28*, 134–146. e134.
- (28) O'Reilly, C.; Grimaud, G. M.; Coakley, M.; O'Connor, P. M.; Mathur, H.; Peterson, V. L.; O'Donovan, C. M.; Lawlor, P. G.; Cotter, P. D.; Stanton, C.; Rea, M. C.; Hill, C.; Ross, R. P. Modulation of the gut microbiome with nisin. *Sci. Rep.* **2023**, *13*, No. 7899.
- (29) Li, P.; Li, M.; Wu, T.; Song, Y.; Li, Y.; Huang, X.; Lu, H.; Xu, Z. Z. Systematic evaluation of antimicrobial food preservatives on glucose metabolism and gut microbiota in healthy mice. *NPJ Sci. Food* **2022**, *6*, 42.
- (30) Draper, L. A.; Cotter, P. D.; Hill, C.; Ross, R. P. Lantibiotic resistance. *Microbiol. Mol. Biol. Rev.* **2015**, *79*, 171–191.
- (31) Hatzioanou, D.; Gherghisan-Filip, C.; Saalbach, G.; Horn, N.; Wegmann, U.; Duncan, S. H.; Flint, H. J.; Mayer, M. J.; Narbad, A. Discovery of a novel lantibiotic nisin O from *Blautia obeum* A2–162, isolated from the human gastrointestinal tract. *Microbiology* **2017**, *163*, 1292–1305.
- (32) Wiedemann, I.; Breukink, E.; van Kraaij, C.; Kuipers, O. P.; Bierbaum, G.; de Kruijff, B.; Sahl, H. G. Specific binding of nisin to the peptidoglycan precursor lipid II combines pore formation and inhibition of cell wall biosynthesis for potent antibiotic activity. *J. Biol. Chem.* **2001**, *276*, 1772–1779.
- (33) Yuan, J.; Zhang, Z. Z.; Chen, X. Z.; Yang, W.; Huan, L. D. Site-directed mutagenesis of the hinge region of nisin Z and properties of nisin Z mutants. *Appl. Microbiol. Biotechnol.* **2004**, *64*, 806–815.
- (34) Hasper, H. E.; de Kruijff, B.; Breukink, E. Assembly and stability of nisin-lipid II pores. *Biochemistry* **2004**, *43*, 11567–11575.
- (35) Field, D.; Connor, P. M.; Cotter, P. D.; Hill, C.; Ross, R. P. The generation of nisin variants with enhanced activity against specific gram-positive pathogens. *Mol. Microbiol.* **2008**, *69*, 218–230.
- (36) O'Connor, M.; Field, D.; Grainger, A.; O'Connor, P. M.; Draper, L.; Ross, R. P.; Hill, C. Nisin M: a bioengineered nisin A variant that retains Full induction capacity but has significantly reduced antimicrobial activity. *Appl. Environ. Microbiol.* **2020**, *86*, No. e00984-20, DOI: 10.1128/AEM.00984-20.
- (37) Cruz, L.; Garden, R. W.; Kaiser, H. J.; Sweedler, J. V. Studies of the degradation products of nisin, a peptide antibiotic, using capillary electrophoresis with off-line mass spectrometry. *J. Chromatogr. A* **1996**, *735*, 375–385.
- (38) Barbour, A.; Smith, L.; Oveisi, M.; Williams, M.; Huang, R. C.; Marks, C.; Fine, N.; Sun, C.; Younesi, F.; Zargar, S.; Oruganty, R.; Horvath, T. D.; Haidacher, S. J.; Haag, A. M.; Sabharwal, A.; Hinz, B.; Glogauer, M. Discovery of phosphorylated lantibiotics with proimmune activity that regulate the oral microbiome. *Proc. Natl. Acad. Sci. U.S.A.* **2023**, *120* (22), No. e2219392120, DOI: 10.1073/pnas.2219392120.
- (39) Lowe, T. M.; Chan, P. P. tRNAscan-SE On-line: integrating search and context for analysis of transfer RNA genes. *Nucleic Acids Res.* **2016**, *44*, W54–57.
- (40) Chan, P. P.; Lin, B. Y.; Mak, A. J.; Lowe, T. M. tRNAscan-SE 2.0: improved detection and functional classification of transfer RNA genes. *Nucleic Acids Res.* **2021**, *49*, 9077–9096.
- (41) Wu, C.; van der Donk, W. A. Engineering of new-to-nature ribosomally synthesized and post-translationally modified peptide natural products. *Curr. Opin. Biotechnol.* **2021**, *69*, 221–231.
- (42) Yang, X.; van der Donk, W. A. Ribosomally synthesized and post-translationally modified peptide natural products: new insights into the role of leader and core peptides during biosynthesis. *Chem. – Eur. J.* **2013**, *19* (24), 7662–7677, DOI: 10.1002/chem.201300401.
- (43) Li, B.; Yu, J. P.; Brunzelle, J. S.; Moll, G. N.; van der Donk, W. A.; Nair, S. K. Structure and mechanism of the lantibiotic cyclase involved in nisin biosynthesis. *Science* **2006**, *311*, 1464–1467.
- (44) Zhang, Z. J.; Lehmann, C. J.; Cole, C. G.; Pamer, E. G. Translating microbiome research from and to the clinic. *Annu. Rev. Microbiol.* **2022**, *76*, 435–460.
- (45) Peschel, A.; Otto, M.; Jack, R. W.; Kalbacher, H.; Jung, G.; Götz, F. Inactivation of the *dlt* operon in *Staphylococcus aureus* confers sensitivity to defensins, protegrins, and other antimicrobial peptides. *J. Biol. Chem.* **1999**, *274*, 8405–8410.
- (46) McBride, S. M.; Sonenshein, A. L. The *dlt* operon confers resistance to cationic antimicrobial peptides in *Clostridium difficile*. *Microbiology* **2011**, *157*, 1457–1465.
- (47) Draper, L. A.; Grainger, K.; Deegan, L. H.; Cotter, P. D.; Hill, C.; Ross, R. P. Cross-immunity and immune mimicry as mechanisms of resistance to the lantibiotic lactacin 3147. *Mol. Microbiol.* **2009**, *71*, 1043–1054.
- (48) Draper, L. A.; Tagg, J. R.; Hill, C.; Cotter, P. D.; Ross, R. P. The *spiFEG* locus in *Streptococcus infantarius* subsp. *infantarius* BAA-102 confers protection against nisin U. *Antimicrob. Agents Chemother.* **2012**, *56*, 573–578.
- (49) Starón, A.; Finkeisen, D. E.; Mascher, T. Peptide antibiotic sensing and detoxification modules of *Bacillus subtilis*. *Antimicrob. Agents Chemother.* **2011**, *55*, 515–525.
- (50) Collins, B.; Joyce, S.; Hill, C.; Cotter, P. D.; Ross, R. P. TelA contributes to the innate resistance of *Listeria monocytogenes* to nisin and other cell wall-acting antibiotics. *Antimicrob. Agents Chemother.* **2010**, *54*, 4658–4663, DOI: 10.1128/AAC.00290-10.
- (51) Thedieck, K.; Hain, T.; Mohamed, W.; Tindall, B. J.; Nimtz, M.; Chakraborty, T.; Wehland, J.; Jänsch, L. The MprF protein is required for lysinylation of phospholipids in listerial membranes and confers resistance to cationic antimicrobial peptides (CAMPs) on *Listeria monocytogenes*. *Mol. Microbiol.* **2006**, *62*, 1325–1339.
- (52) Sun, Z.; Zhong, J.; Liang, X.; Liu, J.; Chen, X.; Huan, L. Novel mechanism for nisin resistance via proteolytic degradation of nisin by the nisin resistance protein NSR. *Antimicrob. Agents Chemother.* **2009**, *53*, 1964–1973.
- (53) Khosa, S.; Alkhatib, Z.; Smits, S. H. NSR from *Streptococcus agalactiae* confers resistance against nisin and is encoded by a conserved *nsr* operon. *Biol. Chem.* **2013**, *394*, 1543–1549.
- (54) Stein, T.; Heinzmann, S.; Solovieva, I.; Entian, K. D. Function of *Lactococcus lactis* nisin immunity genes *nisI* and *nisFEG* after coordinated expression in the surrogate host *Bacillus subtilis*. *J. Biol. Chem.* **2003**, *278*, 89–94.
- (55) Wang, X.; van Beekveld, R. A. M.; Xu, Y.; Parmar, A.; Das, S.; Singh, I.; Breukink, E. Analyzing mechanisms of action of antimicrobial peptides on bacterial membranes requires multiple complementary assays and different bacterial strains. *Biochim. Biophys. Acta, Biomembr.* **2023**, *1865*, No. 184160, DOI: 10.1016/j.bba-mem.2023.184160.
- (56) Garreth, W. L.; Enriqueta, G. G.; Calum, J. W.; Paula, M. O. C.; Máire, B.; Paul, D. C.; Cairtriona, M. G. Nisin G is a novel nisin variant produced by a gut-derived *Streptococcus salivarius* bioRxiv 20222022-02 DOI: 10.1101/2022.02.15.480493.
- (57) Garcia-Gutierrez, E.; O'Connor, P. M.; Saalbach, G.; Walsh, C. J.; Hegarty, J. W.; Guinane, C. M.; Mayer, M. J.; Narbad, A.; Cotter, P. D. First evidence of production of the lantibiotic nisin P. *Sci. Rep.* **2020**, *10*, No. 3738.
- (58) Sevillano, E.; Peña, N.; Lafuente, I.; Cintas, L. M.; Muñoz-Atienza, E.; Hernández, P. E.; Borrero, J.; Nisin, S. a novel nisin variant produced by *Ligilactobacillus salivarius* P1CEA3. *Int. J. Mol. Sci.* **2023**, *24* (7), 6813 DOI: 10.3390/ijms24076813.
- (59) Christophers, M.; Heng, L.; Heng, N.; Nisin, E. a new nisin variant produced by *Streptococcus equinus* MDC1. *Appl. Sci.* **2023**, *13* (2), 1186 DOI: 10.3390/app13021186.
- (60) Hasper, H. E.; Kramer, N. E.; Smith, J. L.; Hillman, J. D.; Zachariah, C.; Kuipers, O. P.; de Kruijff, B.; Breukink, E. An alternative bactericidal mechanism of action for lantibiotic peptides that target lipid II. *Science* **2006**, *313*, 1636–1637.
- (61) Etayash, H.; Azmi, S.; Dangeti, R.; Kaur, K. Peptide Bacteriocins - Structure Activity Relationships. *Curr. Top. Med. Chem.* **2016**, *16*, 220–241.

(62) Hsu, S. T.; Breukink, E.; Tischenko, E.; Lutters, M. A.; De Kruijff, B.; Kaptein, R.; Bonvin, A. M.; Van Nuland, N. A. The nisin-lipid II complex reveals a pyrophosphate cage that provides a blueprint for novel antibiotics. *Nat. Struct. Mol. Biol.* **2004**, *11*, 963–967.

(63) Medeiros-Silva, J.; Jekhmane, S.; Paioni, A. L.; Gawarecka, K.; Baldus, M.; Swiezewska, E.; Breukink, E.; Weingarth, M. High-resolution NMR studies of antibiotics in cellular membranes. *Nat. Commun.* **2018**, *9*, No. 3963.